Neuron, Vol. 28, 431–441, May, 2000, Copyright ©2000 by Cell Press

A Critical Role for a Rho-Associated Kinase, p160ROCK, in Determining Axon Outgrowth in Mammalian CNS Neurons

Haruhiko Bito,*§ Tomoyuki Furuyashiki,* Hisamitsu Ishihara,† Yoshikazu Shibasaki,† Kazumasa Ohashi,‡ Kensaku Mizuno,‡ Midori Maekawa,* Toshimasa Ishizaki,* and Shuh Narumiya*

*Department of Pharmacology
Kyoto University Faculty of Medicine
Sakyo-ku, Kyoto 606-8315
†Department of Metabolic Diseases
Graduate School of Medicine
University of Tokyo
Bunkyo-ku, Tokyo 113-8655
‡Biological Institute
Graduate School of Science
Tohoku University
Sendai 980-8578
Japan

Summary

We tested the contribution of the small GTPase Rho and its downstream target p160ROCK during the early stages of axon formation in cultured cerebellar granule neurons. p160ROCK inhibition, presumably by reducing the stability of the cortical actin network, triggered immediate outgrowth of membrane ruffles and filopodia, followed by the generation of initial growth cone–like membrane domains from which axonal processes arose. Furthermore, a potentiation in both the size and the motility of growth cones was evident, though the overall axon elongation rate remained stable. Conversely, overexpression of dominant active forms of Rho or ROCK was suggested to prevent initiation of axon outgrowth. Taken together, our data indicate a novel role for the Rho/ROCK pathway as a gate critical for the initiation of axon outgrowth and the control of growth cone dynamics.

Introduction

Formation of appropriate connections between neurons is a prerequisite for the establishment and maturation of neural circuits. Determination of cell fate, neuronal migration and synaptic wiring must proceed in a sequential and coordinated fashion, following a unique program based upon genetic information and local gradients of extracellular guidance cues (Goodman and Shatz, 1993; Goodhill, 1998). While many key players implicated in these events have recently been identified (Culotti and Kolodkin, 1996; Tessier-Lavigne and Goodman, 1996; Van Vactor and Flanagan, 1999), it remains largely unknown how neurons are able to discriminate and decode from multiple coexisting sources of extracellular cues. Furthermore, little is yet known about the intracellular molecular machinery allowing neurons to faithfully translate extracellular signals into a predetermined set of coherent, spatiotemporally orchestrated, phenotypic responses that involve long-term changes in cell morphology and gene expression.

Because axon outgrowth is one of the first distinguishable neuron-specific events that follow terminal differentiation of neuronal precursors into neurons, and because appropriate axon pathfinding is crucial for proper formation of functional synapses and circuits, the molecular basis for axonal growth has received much attention and has been investigated extensively. Recent genetic work in fruit flies, worms, and mice, as well as studies using cultured neuronal cells, pointed to the importance of Rho family small GTPases in the regulation of neuronal migration, neuritogenesis, axon pathfinding, and growth cone signaling (Luo et al., 1994, 1996; Sone et al., 1997; Threadgill et al., 1997; Zipkin et al., 1997; Albertinazzi et al., 1998; Nikolic et al., 1998; Steven et al., 1998). However, the downstream events following GTPase activation are poorly described.

Here, we have examined in detail the contribution of a Rho-dependent serine/threonine protein kinase, p160ROCK (Ishizaki et al., 1996; Leung et al., 1996; Matsui et al., 1996; Narumiya et al., 1997), as a potential regulator of axonogenesis downstream of Rho in the context of the cerebellar granule neuron, a neuronal cell type of the CNS, for which the sequence of events from entry into postmitotic phase, neuronal migration, neuritogenesis, and synaptogenesis is well described, both in vivo and in culture (Altman and Bayer, 1996; Hatten, 1999). Transient transfection using GFP as a morphological tracer revealed that up- and downregulation of the Rho/ROCK pathway in cultured cerebellar granule neurons, during the first day in vitro (div), strongly affected axon numbers and growth cone sizes but much less the axon length. Close examination of the effect of Y-27632, a specific ROCK inhibitor (Uehata et al., 1997), indicated that inhibition of endogenous ROCK not only was sufficient to initiate formation of exuberant axonal processes but also seemed to facilitate axonal maturation during the very early stages of axonogenesis, while largely sparing axon elongation. Furthermore, in addition to its function during early axon outgrowth, ROCK was shown to negatively control the size and the motility of axonal growth cones at the tip of extending axons. Thus, the Rho/ROCK-mediated negative regulation on actin dynamics at the soma and in the growth cones may be critical to regulate axon formation and may help determine the accuracy and the exact timing/number of axonal outputs from an immature neuronal somata.

Results

Rho/p160ROCK Pathway Regulates the Number of Axons during Early Axonogenesis in Dissociated Cerebellar Granule Cell Culture

To specifically test the role for Rho-mediated signaling during axonogenesis, we made use of a cerebellar granule cell preparation, where axonogenesis progressively

§To whom correspondence should be addressed (e-mail: hbito@mfour.med.kyoto-u.ac.jp).

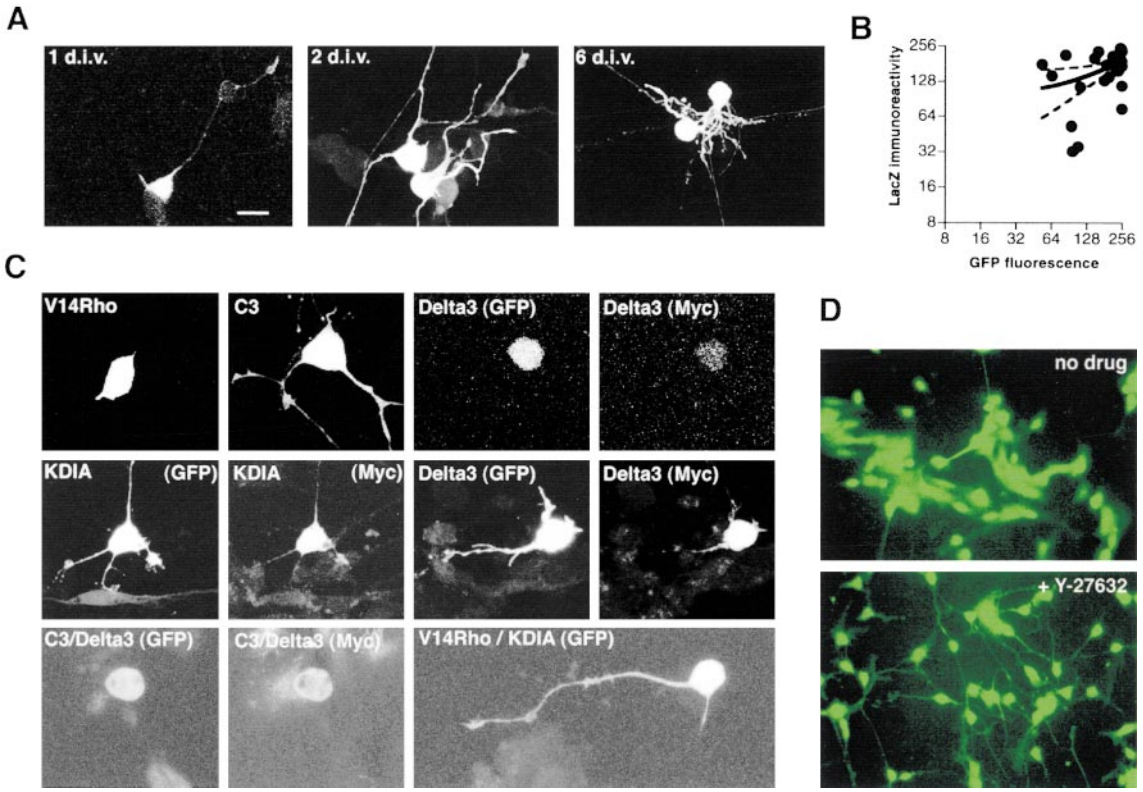

Figure 1. Axonogenesis Is Affected by Overexpressing Rho/ROCK Mutants in Cerebellar Granule Neurons

(A) Axonogenesis precedes dendritogenesis, as visualized using GFP as a morphological marker. Shorter and thicker dendrites are generated only after 2 div, in the vicinity of the cell body. Scale bar, 10 μm.

(B) Efficacy of cotransfection. Comparison of cotransfected LacZ immunoreactivity with GFP fluorescence showed a clear linear correlation (solid line; 95% confidence interval shown by dotted lines), with most data points accumulated in the right upper quadrant.

(C) Phenotypes of neurons expressing various Rho/ROCK mutants. See text for detail. While the majority of V14Rho- or ROCK-Delta3-expressing neurons lacked neurites, the minority that expressed axons showed normal extension. One such example is shown for Delta3 (right middle images).

(D) Inhibition of ROCK using Y-27632 (10 μM) was sufficient to promote axonogenesis during the first div, as shown by the rise in tau-immunopositive (green) neurites.

occurred during the first several days and preceded the development of far shorter dendrites, which only began at 2 or 3 div (Figure 1A), in keeping with previous reports (Powell et al., 1997). Using a lipid-based transfection method, cotransfection of GFP cDNA along with other cDNAs was reliably achieved (Figure 1B). Thus, axonal growth in very young neurons could be visualized as early as 18–24 hr after plating, making it possible to test the effect of mutants and modifiers of the Rho pathway (Figures 1C and 2A). When a dominant active form of RhoA (V14Rho) was cotransfected with GFP, V14Rho-expressing neurons bore few neurites, if any, 18 hr after plating. In contrast, cells coexpressing C3, a RhoA-inhibiting enzyme, possessed an increased number of processes.

We next tested the involvement of p160ROCK, a Rho-associated serine/threonine kinase. We initially found that treatment with Y-27632, a specific inhibitor of p160ROCK, not only was sufficient by itself to reproduce the C3 effect but was also able to rescue the defect in axon outgrowth in V14Rho-transfected neurons (Figure 2A). Overexpression of a constitutive active ROCK-Delta3 induced a significant reduction in process number, similar to V14Rho (Figure 2A, Delta3). Transfection of a RhoA binding–defective and kinase-dead construct of ROCK, which works as a dominant negative form of ROCK, induced a converse phenotype with a significantly increased number of axons (Figures 1C and 2A, KDIA), in accord with the C3 effect. Finally, cotransfection experiments (V14Rho with KDIA or C3 with Delta3) showed that the phenotype of the ROCK mutants dominated over the effect of Rho manipulation, supporting the notion that ROCK lies downstream of Rho in the control of axon numbers (Figure 2B).

During all these experiments, the axon length was also monitored (Figures 2A and 2B). Only C3 expression caused a statistically significant increase in axon length compared to the control, while all other manipulations showed no significant effect, despite dramatic alterations in the axon numbers in some cases. For instance, while V14Rho and Delta3 both strongly reduced axon numbers, the mean length of the prevailing axons was unchanged (see Figure 1C, Delta3, for an example of an atypical Delta3-expressing neuron with preserved neurites). Thus, we failed to find a direct link between Rho/ROCK activity and the resulting axon length.

To rule out the possibility that our data were confounded by the transfection procedure itself, we tested

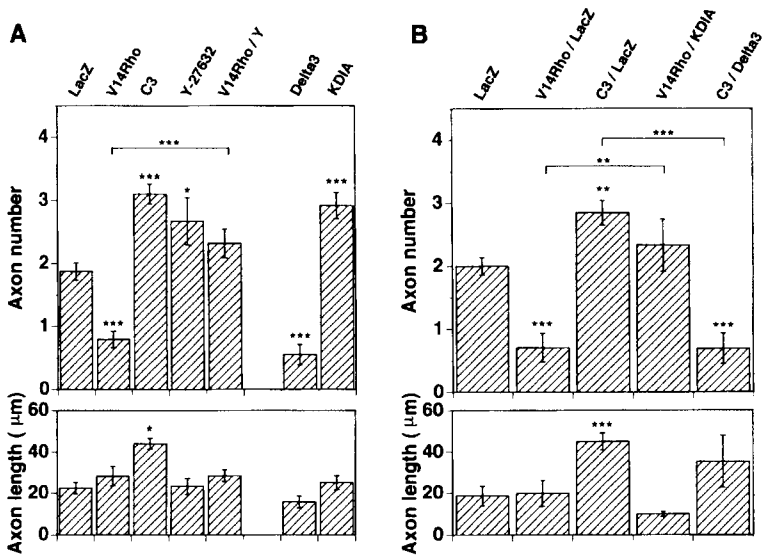

Figure 2. Bidirectional Regulation of Axon Number by Rho/ROCK Activity in Cerebellar Granule Neurons

(A) Quantitative analyses of the axonal phenotypes induced by overexpression of Rho/ROCK mutant plasmids.

(B) Combined transfection reveals that ROCK is a functional Rho effector implicated in regulation of axon number (*$p < 0.05$, **$p < 0.01$, ***$p < 0.001$, in comparison to the LacZ controls, unless otherwise indicated).

the effect of Y-27632 on naive untransfected neurons during the first div. The number of tau immunoreactivity (IR) -positive axonal processes was augmented drastically (Figure 1D), confirming our transfection results.

These results thus pointed to the possibility that ROCK may be a critical Rho effector that regulates and limits axon numbers during early axonogenesis.

Direct Observation of the Initial Stages of Axon Formation Demonstrates a Link between ROCK-Regulated Actin Dynamics and the Prevention of Precocious Induction of Polarity and Axonal Processes

We next measured the consequence of Y-27632-mediated ROCK inhibition during the earliest stages of axon formation in vitro. Cells were initially loaded with the vital membrane dye PKH-26 (Rivas and Hatten, 1995) and further stained with Oregon Green–phalloidin, to monitor the time-dependent changes in both the somatic membrane shapes and intracellular F-actin distribution (Figure 3A). In the control, a gradual gain in cell polarity resulted in the formation of the earliest growth cone–like structures at around 6 hr after plating, leading to a bipolar process formation at 12 hr (Figure 3A, left images). In the Y-27632-treated cells, however, 3 min was usually sufficient to destabilize the integrity of the cortical actin network and trigger the generation of the first membrane ruffles and filopodia (Figure 3A, right images). Subsequently, some membrane patches began to protrude and generate processes with enlarged growth cone–like structures as early as 1.5–3 hr after plating. More than three of these processes were usually seen for each soma in the Y-27632-treated cells. While extension of the processes started earlier than in the controls, we did not see an overwhelming change in the average length of the processes per each cell body at 12 hr.

Quantitative analyses of these observations suggested that while the majority of untreated cells gained a process (either a filopodia or an axon) over several hours, a mere 3 min treatment was sufficient to generate the first processes in the presence of Y-27632 (Figure 3B, solid lines). The total number of observed processes was by and large stable over the period of observation, indicating that the major increment in process number occurred immediately after ROCK inhibition (Figure 3B). In contrast to filopodia, which were filled with F-actin only, processes longer than 3 μm in length could be distinguished as a more mature entity containing tubulin-IR also (data not shown). Treatment with Y-27632 strongly facilitated the transition from filopodia to microtubule-containing axonal processes during the earliest hours (Figure 3C). With regard to the mean process length, an initial difference in favor of the drug-treated group was dissipated at the end of the experiments, indicating that the axon elongation rate per se was not systematically altered during ROCK inhibition (Figure 3D).

These data suggested that ROCK inhibition may affect the integrity of the actin network at the somatic cortices during the earliest stages of axonogenesis. This event in turn seemed to be sufficient to trigger a precocious initiation of process formation.

To confirm this interpretation, we repeated the same experiment and continuously monitored the changes in membrane dynamics in PKH-26-loaded single cells, using time-lapse laser confocal microscopy (Figure 4A). In control cells, polarity formation in membrane structures was slowly initiated and small ruffles were usually formed during the first few hours (Figure 4A, lower images). In contrast, a majority of cells gained several dynamically moving filopodial extensions even before the beginning of the confocal measurements, within a couple of minutes after starting Y-27632 treatment. In one example where the cell attachment was apparently looser, the recording of a drastic shape transition from round-and-smooth to polygonal-with-filopodia was achieved: the shape shift occurred within minutes, starting at frame 32′ (Figure 4A, upper images). After these initial steps, the growth cone–like extended membrane domains became the origins of axonal processes within a few hours.

Finally, to further evaluate the significance of such

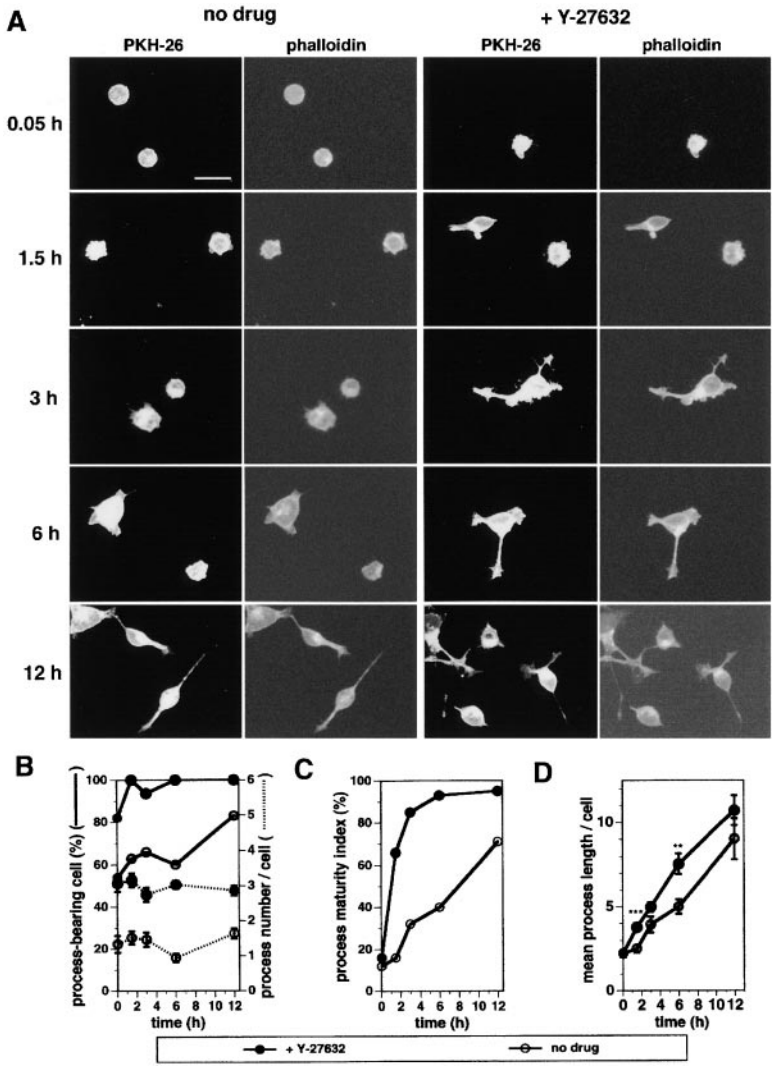

Figure 3. ROCK Inhibition Strongly Affects the Integrity of Cortical Actin Morphology, Which in Turn Leads to Formation of Precocious Neuronal Polarity and Exuberant Axons, While Sparing Axon Extension

(A) Time profile of Y-27632 (10 μM) -induced changes in F-actin distribution and membrane morphology. ROCK-inhibited neurons display larger numbers of filopodia, membrane ruffles, growth cones, and axonal processes. Axon elongation, while starting earlier in Y-27632-treated cells, seems to reach comparable levels in the control group after 12 hr. To equalize all incubation conditions across coverslips within an experiment, all cells were incubated in the presence or absence of the drug and were serially fixed at indicated time points. PKH-26 stains indicate the intracellular and plasma membranes and Oregon Green–conjugated phalloidin was used to visualize F-actin distribution. Scale bar, 10 μm.

(B) Process formation in the drug-treated groups occurs within minutes. The total number of processes was not dramatically altered during the course of the experiments.

(C) Facilitation of the transition of microtubule-free filopodia into axons by Y-27632. The process maturity index was calculated as the percentage of neurites over 3 μm among all detectable neurites, based upon the finding that only larger neurites contained microtubules, and that the cut-off was usually 3 μm.

(D) Lack of a predominant change in axon elongation rate. While the length of Y-27632-treated axons stayed slightly higher up to 6 hr, due to the earlier axon initiation, the accumulated length was unchanged from controls later on.

Rho/ROCK involvement in axon initiation, we turned to a reaggregate culture of cerebellar granule neurons, in which neurons are able to extend axons out of the center of the reaggregates (Lindner et al., 1985; Gao et al., 1991). We tested the time dependence of the Y-27632 effect on axonal outgrowth, as measured by GAP-43-IR, a marker enriched preferentially in growth cones and in axonal membranes. As shown in Figure 4B, inhibition of the Rho/ROCK pathway, either by bath application of C3 exoenzyme or Y-27632, strongly enhanced the number of GAP-43-IR-positive processes as early as 6 hr or 12 hr after plating. However, the difference in GAP-43-IR density apparently dissipated at 36 hr after replating of reaggregates. These results are consistent with the idea that endogenous ROCK activity mediates a critical step in the control of actin dynamics that may help prevent the formation of precocious polarity and of aberrant axonal processes, during the very early hours of axonogenesis.

The Rho/ROCK Pathway Regulates the Size and the Dynamics of Axonal Growth Cones

Growth cones are particularly active during the first day in culture, and previous reports have indeed suggested an important contribution of RhoGTPases in the regulation of actin in the growth cones (Gallo and Letourneau, 1998). During this work, we noticed that the growth cone sizes might reflect the state of Rho/ROCK activity in a neuron, indicating that the Rho/ROCK pathway may also serve as a gate that controls the size of the growth cones at the tips of a growing axon, independently from its function on axon initiation. Costaining of F-actin and tubulin in the growth cones revealed that Y-27632-mediated ROCK inhibition generated a proliferation of actin meshwork within almost all growth cones that was accompanied with the entry of microtubule bundles (Figures 5C [inset] and 5E).

We further examined the size of growth cones in transfected cerebellar granule cells, 18 hr after plating (Figures 6A and 6B). V14Rho significantly reduced the size of growth cones, while C3 expression or application of the ROCK inhibitor dramatically augmented it. In contrast, the size of the cell body in the same neurons was not altered as prominently, suggesting that the growth cone structure was a particularly sensitive discriminator of Rho activity (data not shown). The phenotype in V14Rho-transfected neurons was rescued by bath appli-

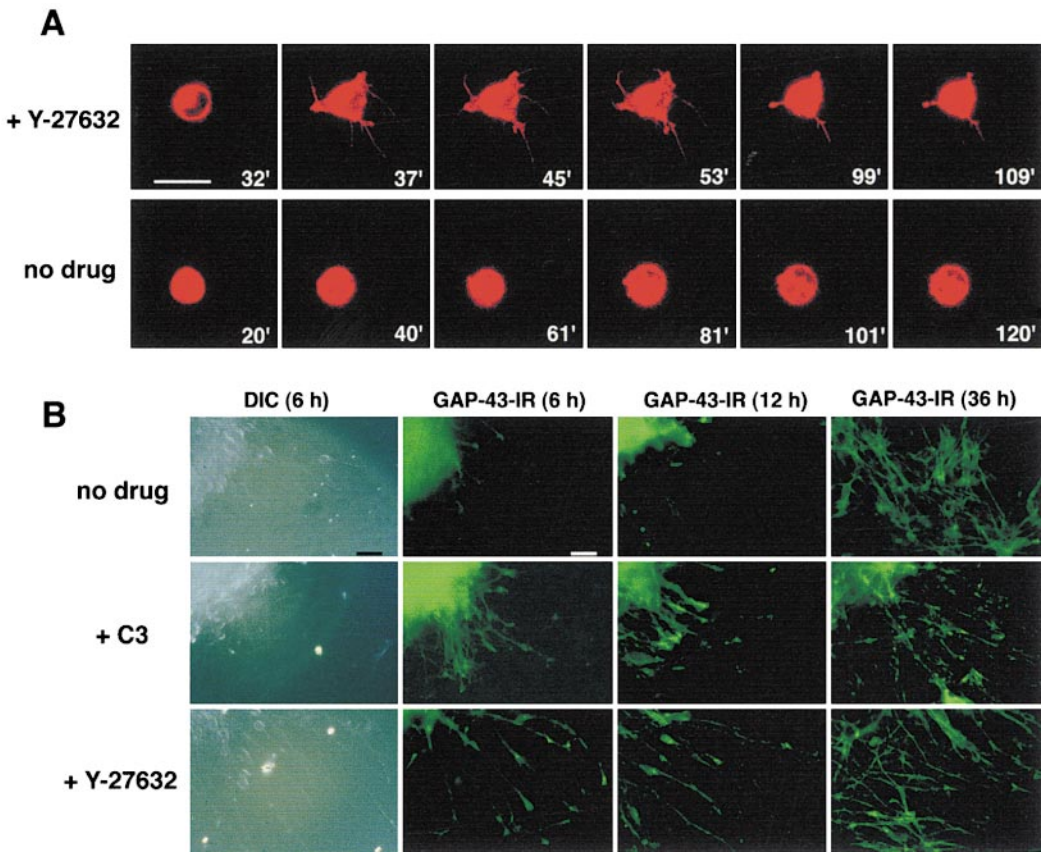

Figure 4. Early Facilitation of Axon Initiation by Y-27632

(A) Single-cell imaging demonstrates that pharmacological inhibition of ROCK activity using Y-27632 (10 μM) dramatically triggers neuronal polarity formation at very early time points. This further indicates that all mechanisms for axon formation are present at the time of plating, but that endogenous Rho/ROCK activity prevents this event from occurring until a later stage in the normal course of axon development. The time after the start of the recording is indicated. Note that a certain amount of asymmetry, though rather subtle, is achieved even in the untreated cells after a couple of hours. Scale, 10 μm.

(B) Pharmacological inhibition of Rho/ROCK pathway promotes axonogenesis during the early hours in a reaggregate culture. The extension of axons was sequentially monitored at 6 hr, 12 hr, and 36 hr, in the absence or presence of extracellular C3 exoenzyme (30 μg/ml) or Y-27632 (10 μM) in the bath solution, using GAP-43-IR (green). The higher sensitivity seen in the early hours suggested that endogenous Rho/ROCK activity was elevated during this period and prevented initiation of axons. Scale bar, 20 μm.

cation of Y-27632 or cotransfection of KDIA, and dominant ROCK mutations reversed the effect of manipulating Rho activity to the opposing direction, indicating that ROCK may also play a critical role in the regulation of growth cone size downstream of Rho (Figures 6A and 6B).

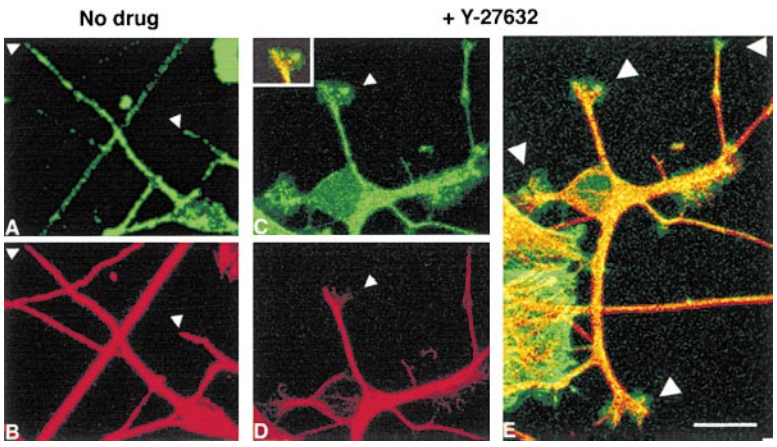

Figure 5. Changes in the Cytoskeletal Structures Accompanies the Aberrant Enlargement in Growth Cones Induced by ROCK Inhibition

(A and B) Extension of both F-actin (A) and microtubules (B) up to the tip of the axon in a control cell (1 div) with little growth cones (shown by arrowheads).

(C–E) Giant growth cones (shown by arrowheads) in Y-27632-treated cerebellar granule cell (1 div) are filled with an exuberant amount of F-actin stain (C), accompanied by invasion of several microtubule bundles (D). An overlay of the two stains are shown as an inset in (C) or as (E). Scale bar, 12.5 μm.

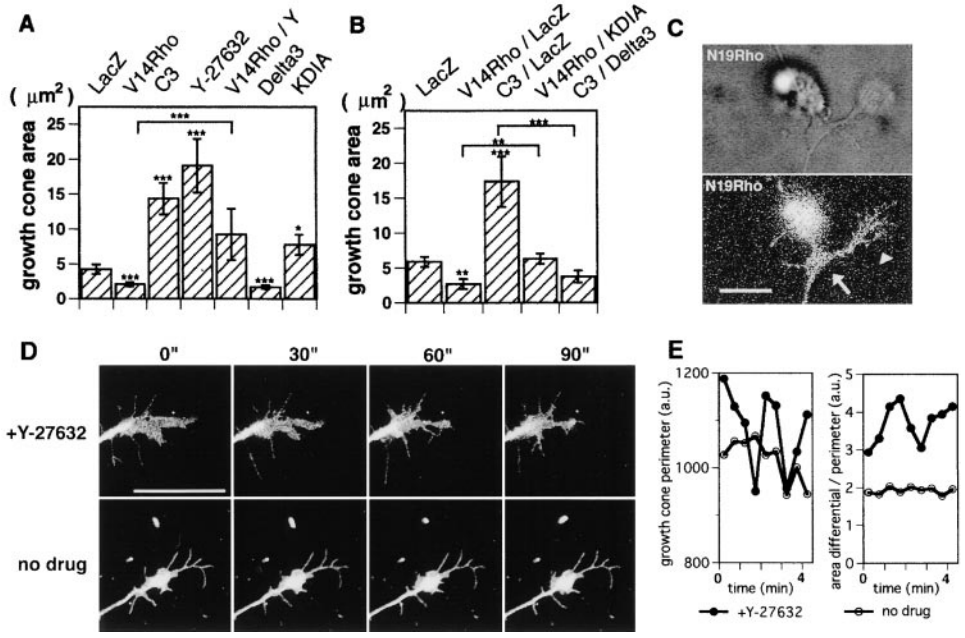

Figure 6. Negative Regulation of Growth Cone Size and Motility by ROCK

(A and B) Bidirectional regulation of growth cone size by Rho/ROCK activity during the first div. See text for detail (*$p < 0.05$, **$p < 0.01$, ***$p < 0.001$, in comparison to the LacZ controls, unless otherwise indicated).

(C) Detection of PKH-26 stain in the enlarged growth cones using confocal microscopy. An N19Rho-infected dissociated cerebellar granule cell (2 div) was visualized live. Note that the fluorescent channel (bottom) can better record the fine details of the filopodial extensions (arrowhead) at the tip of the growth cone (arrow), compared to the DIC image (top). Scale bar, 10 μm.

(D) Live imaging of growth cone dynamics. Time-lapse confocal images were acquired in the absence or presence of Y-27632 (10 μM). Compared to the nontreated cells, growth cones in ROCK-inhibited neurons revealed an extended leading edge with higher motility during the whole period of image acquisition. Scale bar, 10 μm.

(E) Quantification of the motility of the growth cones in the same series of image sequences as the data shown in (D).

The increase in growth cone area by Rho/ROCK inhibition may either result from an irreversible enlargement of the tip of the axonal process, or from a transient release of the control of growth cone dynamics. To distinguish between these two possibilities, we recorded the live behavior of axonal growth cones using time-lapse confocal microscopy. Increase in laser power was sufficient to visualize the behavior of live PKH-26-stained growth cones, as illustrated in the experiments where neurons were infected with a dominant negative Rho-expressing virus (Figure 6C). Spontaneous formation and retraction of filopodia-like structures were observed in the presence or absence of Y-27632 throughout the recording period (Figure 6D), indicating that ROCK activity may not be implicated in controlling the appearance or disappearance of these structures. However, Y-27632 treatment, in addition to causing a tonic expansion of the perimeter of the growth cone, induced a significant increase in the motility of the growth cone membranes and the rate of turnover of filopodia-like microprocesses (Figure 6E). Thus, the Rho/ROCK pathway was likely to control not only the size but also the dynamic instability of the growth cone membranes.

Involvement of Multiple ROCK Substrates, Including LIM Kinase, in the Control of Axonogenesis

We finally asked what substrate(s) may mediate the ROCK-dependent control of the actin network in the cell soma and in the growth cones of cerebellar granule neurons during axonogenesis. We recently discovered that LIM kinase-1 (LIMK-1) was a substrate for p160ROCK in N1E-115 cells (Maekawa et al., 1999; Ohashi et al., 2000). LIMK-1 has received much attention lately, since its gene locus was linked with impaired visuospatial constructive cognition in Williams syndrome (Frangiskakis et al., 1996; Tassabehji et al., 1996), and it was found that LIMK-1 phosphorylated Ser-3 of cofilin, an important regulator of actin dynamics in many cell types, in a Rho family GTPase-dependent manner (Arber et al., 1998; Yang et al., 1998; Edwards et al., 1999; Sumi et al., 1999). We therefore tested whether overexpression of wild-type LIMK-1 (wtLIMK) or its kinase-dead mutant (kdLIMK) had any effect on the axon number, axon length, or growth cone size in cerebellar granule cells (Figures 7A and 7B). While wtLIMK only weakly reduced axon number, expression of kdLIMK was sufficient to increase process number close to the level obtained by transfecting dominant negative ROCK (KDIA). The ability of kdLIMK to reverse the effect of constitutive active ROCK-Delta3 suggested that LIMK may in fact act downstream of ROCK. Conversely, wtLIMK failed to impact on the KDIA phenotype at all; however, this may be simply explained by the fact that wtLIMK could not be activated at all in the absence of its own phosphorylation by ROCK, as was recently shown in vitro (Maekawa et al., 1999; Ohashi et al., 2000). Thus, our data were consistent with the idea that LIMK-1 may be a functional substrate for ROCK, in the context

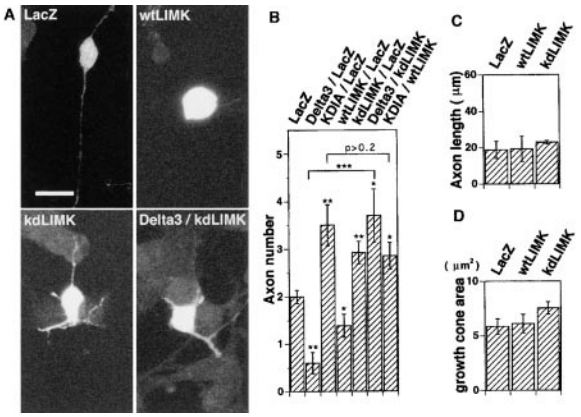

Figure 7. ROCK-Dependent Control of Axonogenesis Is Mediated by Multiple Donwstream Effectors Including, but Not Restricted to, LIM Kinase

(A) Transfection of wild-type (wtLIMK) and kinase-dead (kdLIMK) LIMK-1 cDNA alters axon numbers. Scale bar, 10 μm.

(B) Quantification of the effect of LIMK mutants as compared to phenotypes of ROCK mutants. The effect of kdLIMK dominated over that of Delta3, while the wtLIMK phenotype was not detected in the presence of KDIA, consistent with LIMK lying downstream of a ROCK-dependent phosphorylation event, as suggested by earlier work.

(C) Lack of LIMK effect on axon length.

(D) Lack of LIMK effect on growth cone size. This indicated that a kinase substrate distinct from LIMK-1 may mediate the ROCK effect on growth cone size.

of regulation of axon number. However, no effect was seen with either wtLIMK or kdLIMK, on either axon length or growth cone size, indicating that the ROCK-dependent regulation of growth cone size may be mediated by substrates other than LIMK-1.

These results suggested that multiple ROCK substrates, including, but not restricted to, LIMK-1, may participate in mediating the ROCK effect on the actin cytoskeleton during axon formation.

Discussion

Rho/ROCK Pathway May Function as a Gate Controlling the Initiation of Axon Outgrowth

In this study, we attempted to elucidate the contribution of Rho and Rho targets during axonogenesis in mammalian CNS neurons, using cerebellar granule neurons as a model system. Activation of Rho or ROCK prevented initiation of axon outgrowth, resulting in a significant decrease in the number of axons generated from one neuron. In contrast, inhibition of Rho or ROCK, one of its downstream effectors, induced an apparent multiplication of axonal processes. Furthermore, downregulation of ROCK was sufficient to reduce the stability of the cortical actin network and to immediately promote initiation of neuritogenesis. It should be noted, however, that the combination of active V14Rho and ROCK inhibition (with Y-27632 or KDIA transfection) always yielded a phenotype intermediate between control and C3 levels (Figures 2A and 2B; see also Figures 6A and 6B), thus indicating the possibility that a Rho effector that is not physiologically relevant might nonetheless be activated by exogenous Rho and cooperate with endogenous ROCK in the regulation of axonogenesis.

Taken together, our data indicated that the Rho/ROCK pathway may function as a gate for the initiation of axonogenesis and was actively preventing the induction of instability in the actin cytoskeleton during axonogenesis.

The positive regulators of axon outgrowth include Rac and CDC42 as suggested in other work (Luo et al., 1994, 1996; Kaufmann et al., 1998). Recent studies indicated the possibility that Rho effectors and Rac/CDC42 effectors may crosstalk with each other (Lim et al., 1996; Kozma et al., 1997; Hirose et al., 1998). Our results are consistent with the hypothesis that Rac/CDC42 activities are dominant over Rho once neurites have started to extend, while Rho activity may be more preponderant at the early beginning of neurite formation. This hypothesis is in agreement with the robust effect of ROCK inhibitor Y-27632 on early axonogenesis (Figures 3 and 4). Furthermore, a direct visualization of the earliest steps in axon formation suggested that ROCK activity was specifically implicated in controlling the integrity of the cortical actin network during process initiation (Figure 4A).

Transfection experiments using wild-type and a kinase-dead mutant LIMK-1 suggested an involvement of LIMK-1 as a downstream target of ROCK in the regulation of axon formation. We speculate that during the initial stages of axon outgrowth, the activation of the Rho/ROCK/LIMK-dependent phosphorylation cascade (Maekawa et al., 1999; Ohashi et al., 2000) strongly contributes to maintaining an inactivation state of cofilin and preventing it from being activated by dephosphorylation. When this phosphorylation is counteracted, such as by use of Y-27632 in vitro, or by Rho inhibition in vivo (see below), local accumulation of activated cofilin may indeed trigger a rapid morphological change and generation of neuronal polarity in a Rho-regulated manner (Bradke and Dotti, 1999). Clearly, further work is needed to substantiate this notion. However, it is interesting to note that our finding in a round, process-free neuron under ROCK inhibition corroborates earlier work by Aizawa et al. (1997), who found that nonphosphorylated, active cofilin played a crucial role in the rapid remodeling of the cortical actin meshwork into bundles in *Dictyostelium*.

Minor Effect of Rho/ROCK Perturbation on Axon Elongation

In sharp contrast to the case in neuronal cell lines where application of a Rho/ROCK-activating ligand such as lysophosphatidic acid was sufficient to induce a dramatic retraction of all neurites within minutes and to reverse the neurite elongation process itself (Amano et al., 1998; Hirose et al., 1998; Katoh et al., 1998), neurons overexpressing the active forms of Rho and ROCK could still extend neurites, though these were rarer. Furthermore, expression of synaptic markers occurred normally in Rho/ROCK-activated axons (data not shown). Thus, Rho/ROCK activation in maturing neurons may not counteract and reverse the elongation and maturation of preexisting processes. The high level of expression of microtubules and microtubule-associated proteins in

the axonal process (Figures 1D and 5) was likely to contribute to this sharp dichotomy in the appearance of the Rho/ROCK effect between model cell lines and primary neurons. Thus, the increase in actomyosin contractility induced by higher Rho/ROCK activity may not be sufficient to retract neurites when these already contain a highly organized microtubule structure. Alternatively, we cannot rule out the possibility that the molecular events downstream of ROCK may be regulated in a cell type– or developmental stage–specific manner. In fact, Rho signaling may play distinct biological roles depending on the timing when a regulatory activation or inactivation actually occurs (Sebok et al., 1999).

ROCK May Control the Dynamic Instability of Growth Cones

From a large body of work, growth cone guidance has always been considered as a key continuing process during neuritogenesis where the regulation of actin dynamics was critical (Tanaka and Sabry, 1995). We here tested whether ROCK activity was involved in regulating the shape or the dynamics of growth cones in cerebellar granule neurons. Under ROCK inhibition, the size of growth cones was significantly increased, as was the motility of the growth cone visualized using time-lapse confocal microscopic imaging (Figures 5 and 6), indicating that endogenous ROCK might be involved in the activity-dependent and/or developmentally regulated stabilization of growth cone structures. The increase in the growth cone size during ROCK inhibition was suggested to result, at least in part, from a proliferation of actin meshwork accompanied by abundant invasion of microtubules into the growth cone structures. It is likely that such a mechanism may also be directly involved in regulating the dynamic instability of the leading membrane edge of the growth cones. While an involvement of LIM kinase cannot be totally excluded at this point, we failed to obtain concrete evidence in support of its role in growth cone size regulation. It remains to be determined how other members of the Rho family GTPases, such as Rac and CDC42 or their downstream targets, are implicated in the control of the same processes (Jin and Strittmatter, 1997; Lamoureux et al., 1997).

Physiological Significance of the Rho/ROCK Pathway

Our data lend support to the notion that the Rho/ROCK pathway may function as a gate involved in controlling axon initiation and growth cone dynamics in cerebellar granule neurons. It should be noted, however, that a biologically important role for ROCK at later steps cannot be excluded by any means. In fact, ROCK has been previously reported to form a protein complex with profilin in adult mouse brain lysates, thus strongly indicating an as yet uncharacterized role for ROCK in mature neurons (Witke et al., 1998). Furthermore, Rho may also be involved in regulating other morphogenic processes in neurons such as dendritogenesis or control of dendritic arborization (Ruchhoeft et al., 1999; Lee et al., 2000; Li et al., 2000), as manipulation of Rho or ROCK activity using adenovirus or plasmid transfection induced visible changes in dendrite-like processes in immature hippocampal neurons, cerebellar granule neurons, and young Purkinje cells (H. B. et al., unpublished data). Nakayama et al. (2000) indeed found evidence for a critical role for Rho/ROCK signaling in the maintenance of dendritic complexity in maturing neurons in cultured rat hippocampal slices.

It has been recently shown that upregulation of Rho activity could be constitutively induced by ligand-free p75 low-affinity neurotrophin receptor while its ligand binding abolished Rho activation (Yamashita et al., 1999). Furthermore, Rho activity was reported to be downregulated by cAMP signaling (Busca et al., 1998; Dong et al., 1998; Lang et al., 1996) and activation of NMDA receptors (Li et al., 2000). Thus, the potentiating effect of neurotrophin, cAMP, or neural activity on neurite formation and neuronal development may be mediated, at least in part, by inhibition of the Rho/ROCK pathway: such an event would not only affect the integrity of the cortical actin network, thus favoring neurite outgrowth, but also potentiate both growth cone size and motility. How this could, in turn, possibly alter the growth cone sensitivity to adjacent guidance signals and cues will be a most intriguing question, which clearly should be studied in vivo, within the appropriate cellular context. Additionally, it would be interesting to examine whether there is a similar contribution of ROCK downstream of RhoB during the delamination of neural crest cells from the neural tube (Liu and Jessell, 1998).

A ROCK-dependent mechanism was previously shown to be essential in switching the mode of cell–cell contact occurring between polarized epithelial cells from one type to another (Krendel et al., 1999). Similarly, our own data indicated that Rho-associated kinase p160ROCK, by acting as a potent negative regulator of axon outgrowth and growth cone motility, might play a role as a switch that specifies the timing/number of axons or branching generated from a neuron. Modulation of ROCK activity by Rho and other signaling mechanisms may also alter growth cone size and dynamics, thereby possibly influencing and switching the sensitivity of growth cones toward extracellular signals, perhaps at critical choice points during axon pathfinding and synaptogenesis (Ruchhoeft et al., 1999). Ultimately, the immediate positive effect of ROCK inhibition on filopodia and process formation indicates that a pharmacological intervention to block ROCK activity in neurons may turn out to be a useful therapeutic strategy for treating various kinds of axonopathies such as those induced by nerve injury or diabetes, or to promote axon regeneration (Lehmann et al., 1999).

Experimental Procedures

Neuronal Culture

Culture of CA1/CA3 hippocampal neurons was carried out as described in Bito et al. (1996). For cerebellar granule cell cultures, cerebella were collected from P1–P2 ICR mice, and thin slices were cut in parasagittal directions in ice-cold HANKS(−) (Ca^{2+}-free and Mg^{2+}-free) solution supplemented with 20% fetal calf serum (FCS) (Hyclone). Dissection, centrifugation and plating, and medium changes were essentially carried out as described above for the culture of hippocampal neurons. A detailed protocol can be obtained from the authors upon request.

Reaggregates of cerebellar granule cells were generated by resuspending the final cell pellet in 1 ml of Medium A (Earle's MEM supplemented with 10% FCS, 1 × B-27 [Life Technologies], insulin [25 mg/l, Sigma], glucose [5 g/l], transferrin [100 mg/l, Calbiochem], 2 mM glutamine) in a conical polystyrene centrifugation tube and incubating this in a CO_2 incubator for 24 hr. Reaggregates were then gently plated on a Matrigel coated glass coverslip, left to settle down at room temperature for 30 min, and finally fed with 1 ml of Medium B (Earle's MEM supplemented with 5% FCS, 1 × B-27/insulin [25 mg/l], glucose [5 g/l], transferrin [100 mg/l], 0.5 mM glutamine, 4 μM cytosine arabinoside [Sigma]).

Indirect Immunofluorescent Microscopy and Live PKH-26 Imaging

Immunocytochemistry was performed essentially as described (Bito et al., 1996). Primary and secondary antibodies were as follows: rabbit anti-tau polyclonal (a gift from Y. Ihara, University of Tokyo, 1:1000); mouse anti-GAP-43 (Sigma, 1:200); mouse anti-synaptophysin (Sigma, 1:500); mouse anti-myc (9E10, Santa Cruz, 1:200); mouse anti-α-tubulin (Sigma, 1:200); and FITC-, Texas Red–, or Cy5-conjugated goat anti-rabbit and anti-mouse secondary antibodies (Jackson ImmunoResearch). When necessary, DAPI (100 nM, Molecular Probes) and Oregon Green 488-phalloidin (1:1000, Molecular Probes) were used to stain the nucleus and F-actin, respectively. Live staining using PKH-26 (Sigma) was performed according to the manufacturer's protocol.

Immunofluorescent images were acquired using a BioRad MRC1024 system equipped with a Carl Zeiss AxioVert TV100 microscope and using either an oil-immersed 63× Plan-NEOFLUAR objective (N. A. 1.25) or a 10× ACHROPLAN objective (N. A. 0.25). Individual confocal sections, stacks of Z-scan sections, and time-lapse images were acquired and analyzed using LaserSharp V.3.2 (Bio-Rad). Pseudocolor representations were assembled using Photoshop V5.5 (Adobe). Alternatively, pictures were taken from fixed neurons using a Carl Zeiss Axiophot microscope equipped with a 40× Plan-NEOFLUAR (N. A. 1.30) objective. Live imaging was carried out at 37°C using neurons grown on a custom-made coverslip chamber and placed onto a temperature-controlled Zeiss CO_2 incubator attached to the microscope stage.

Morphometric analyses of GFP-marked neurons were performed using: (1) the MEASURE command in an ARGUS-20 image analysis system (Hamamatsu Photonics) that controls a SIT camera (Hamamatsu Photonics C2400-08) attached to an Axiovert microscope with an 63× Plan-NEOFLUAR objective (N. A. 1.25), or (2) the MEASURE command in the LaserSharp V.3.2 for the MRC-1024. Both methods gave similar results. Initial analysis of transfected neurons were carried out without precise indication of the transfected cDNAs, though the clarity of the phenotype usually compromised the initial lack of knowledge. Neurons with membrane blebbing and fragmented and/or atypical nuclear morphology, and Purkinje cells determined by their characteristic dendritic arbors and large somata (>15 μm) were discarded from all analyses. The length of an axon (distinguished from somatic filopodia ≤3 μm) was defined as the length of the trace from the contour limit of the cell soma (or the aggregate) to the tip of the process. The enlarged area that was present beyond and distal to the thinnest segment at the tip of the axon was considered to be the growth cone. When the diameter of the axon was even or decreased continuously up to the tip of the axon, a circle that fitted the tip was drawn, and its surface area was considered as the growth cone area. Motility of the growth cone within an image sequence was quantified by measuring (1) the area of nonoverlapping regions in the growth cone for each pair of consecutive image frames, and (2) the perimeter of the growth cones, using NIH Image 1.6.2.

Statistical analysis was carried out using Prism 2.0 (Graphpad Software). All data are indicated as means ± SEM. Unpaired t test with Welch's correction was employed to determine statistical significance.

Transfection of Plasmid cDNA Constructs and Infection of Recombinant Adenovirus

Plasmids (pEF-HA-V14Rho [Fujisawa et al., 1998], pCMX-C3 [Fujisawa et al., 1998], ROCK-Delta3 and ROCK-KDIA [Ishizaki et al., 1997], LIMK-WT [wtLIMK], and LIMK-DA [kdLIMK] [Maekawa et al., 1999; Ohashi et al., 2000]) and adenovirus constructs (Myc-N19Rho and Myc-V14Rho adenovirus [Shibasaki et al., 1997]) were as previously described.

Transfection was carried out in the following way, by modifying the last steps of the cell preparation procedure. After adding 3 ml of 20% FCS/HANKS(−) immediately after the trituration, 1 μl of Primary Enhancer Reagent (Stratagene) was added and mixed by gentle tapping. A cell pellet was recovered from a 1000 rpm, 10 min centrifugation at 4°C. For N coverslips subjected to transfection, cells were resuspended in N times the mixture D (80 μl HANKS(−), plasmids 1.3 μg, Lipofectamine 2000 [Life Technologies] 1.3 μl) by pipetting up and down, and N × 20 μl FCS (Hyclone) was finally added. The final cell/plasmids/Lipofectamine 2000 mixture (100 μl) was plated onto φ12 mm round Matrigel (Becton-Dickinson) coated coverslips (Assistent) placed in a 24-well plate. Each coverslip had been coated with 100 μl Matrigel immediately before use. Cells were allowed to settle down for 30 min at room temperature, after which time each coverslip was fed with 0.5 ml of Medium A (same composition as above) in a 24-well plate. Then, for each coverslip subjected to transfection, a 100 μl OptiMEM (Life Technologies) containing 1.3 μg plasmid cDNA and 2 μl Lipofectamine 2000 was added, drop by drop. The plate was incubated in a CO_2 incubator for 8 hr, after which time 0.5 ml of Medium B (same as above) was added per well. The cells were put back into a CO_2 incubator and cultured for another 8–16 hr.

The following details seemed to be important to obtain reliable transfection: transfected plasmids (1.3 μg) consisted of a mixture of 0.3 μg pEGFP-C1 (Clontech) + 1.0 μg plasmid of interest. Mock transfection was carried out using a CMV-LacZ vector. Plasmids were prepared by CsCl ultracentrifugation or using a CONCERT high-purity maxiprep column (Life Technologies). Indicated amounts of plasmid cDNAs and Lipofectamine 2000 were first diluted in half-volumes of OptiMEM or HANKS(−) solutions; plasmid cDNAs were vortexed with the medium for 20 s to maximize the chance of cotransfection of the GFP marker, while Lipofectamine 2000 was diluted by gentle tapping. After a 5 min incubation in separate tubes, plasmids and Lipofectamine 2000 solutions were mixed by gentle tapping in order to generate the final transfection mixture, which was incubated at room temperature for 20–25 min, prior to addition to the culture medium. Under these conditions, usually 10–30 neurons were GFP positive per coverslip at 18 hr after plating and transfection. The number of GFP-expressing neurons significantly increased further, up to 48 hr after transfection. In our hands, the efficacy of cotransfection was >90%.

Acknowledgments

We thank M. Uehata (Yoshitomi Pharmaceuticals) for Y-27632, Y. Ihara (University of Tokyo) for an anti-tau polyclonal antibody, A. Y. Nakayama and L. Luo (Stanford University) for sharing unpublished results, K. Nonomura for technical assistance, and H. Nose and T. Arai for secretarial assistance. This work was supported by Grants-in-Aid from the Ministry of Education, Science, Sports, and Culture of Japan (to H. B., Y. S., K. M., T. I., and S. N.) and grants from the Asahi Glass Research Foundation, the Yamanouchi Foundation for Research on Metabolic Disorders, and the Pharmacopsychiatry Research Foundation (to H. B.). T. F. is a predoctoral fellow from the Japan Society for the Promotion of Science.

Received October 13, 1999; revised April 4, 2000.

References

Aizawa, H., Fukui, Y., and Yahara, I. (1997). Live dynamics of Dictyostelium cofilin suggests a role in remodeling actin latticework into bundles. J. Cell Sci. *110*, 2333–2344.

Albertinazzi, C., Gilardelli, D., Paris, S., Longhi, R., and de Curtis, I. (1998). Overexpression of a neural-specific rho family GTPase, cRac1B, selectively induces enhanced neuritogenesis and neurite branching in primary neurons. J. Cell Biol. *142*, 815–825.

Altman, J., and Bayer, S.A. (1996). The third stage of cerebellar

development: maturation of the cerebellar system. In Development of the Cerebellar System (Boca Raton, FL: CRC Press), pp. 324–524.

Amano, M., Chihara, K., Nakamura, N., Fukata, Y., Yano, T., Shibata, M., Ikebe, M., and Kaibuchi, K. (1998). Myosin II activation promotes neurite retraction during the action of Rho and Rho-kinase. Genes Cells *3*, 177–188.

Arber, S., Barbayannis, F.A., Hanser, H., Schneider, C., Stanyon, C.A., Bernard, O., and Caroni, P. (1998). Regulation of actin dynamics through phosphorylation of cofilin by LIM-kinase. Nature *393*, 805–809.

Bito, H., Deisseroth, K., and Tsien, R.W. (1996). CREB phosphorylation and dephosphorylation: a Ca^{2+}- and stimulus duration–dependent switch for hippocampal gene expression. Cell *87*, 1203–1214.

Bradke, F., and Dotti, C.G. (1999). The role of local actin instability in axon formation. Science *283*, 1931–1934.

Busca, R., Bertolotto, C., Abbe, P., Englaro, W., Ishizaki, T., Narumiya, S., Boquet, P., Ortonne, J.P., and Ballotti, R. (1998). Inhibition of Rho is required for cAMP-induced melanoma cell differentiation. Mol. Biol. Cell *9*, 1367–1378.

Culotti, J.G., and Kolodkin, A.L. (1996). Functions of netrins and semaphorins in axon guidance. Curr. Opin. Neurobiol. *6*, 81–88.

Dong, J.M., Leung, T., Manser, E., and Lim, L. (1998). cAMP-induced morphological changes are counteracted by the activated RhoA small GTPase and the Rho kinase ROKα. J. Biol. Chem. *273*, 22554–22562.

Edwards, D.C., Sanders, L.C., Bokoch, G.M., and Gill, G.N. (1999). Activation of LIM-kinase by Pak1 couples Rac/Cdc42 GTPase signaling to actin cytoskeletal dynamics. Nat. Cell Biol. *1*, 253–259.

Frangiskakis, J.M., Ewart, A.K., Morris, C.A., Mervis, C.B., Bertrand, J., Robinson, B.F., Klein, B.P., Ensing, G.J., Everett, L.A., Green, E.D., et al. (1996). *LIM-kinase1* hemizygosity implicated in impaired visuospatial constructive cognition. Cell *86*, 59–69.

Fujisawa, K., Madaule, P., Ishizaki, T., Watanabe, G., Bito, H., Saito, Y., Hall, A., and Narumiya, S. (1998). Different regions of Rho determine Rho-selective binding of different classes of Rho target molecules. J. Biol. Chem. *273*, 18943–18949.

Gallo, G., and Letourneau, P.C. (1998). Axon guidance: GTPases help axons reach their targets. Curr. Biol. *8*, R80–R82.

Gao, W.O., Heintz, N., and Hatten, M.E. (1991). Cerebellar granule cell neurogenesis is regulated by cell–cell interactions in vitro. Neuron *6*, 705–715.

Goodhill, G.J. (1998). Mathematical guidance for axons. Trends Neurosci. *21*, 226–231.

Goodman, C.S., and Shatz, C.J. (1993). Developmental mechanisms that generate precise patterns of neuronal connectivity. Cell Suppl. *72*, 77–98.

Hatten, M.E. (1999). Central nervous system neuronal migration. Annu. Rev. Neurosci. *22*, 511–539.

Hirose, M., Ishizaki, T., Watanabe, N., Uehata, M., Kranenburg, O., Moolenaar, W.H., Matsumura, F., Maekawa, M., Bito, H., and Narumiya, S. (1998). Molecular dissection of the Rho-associated protein kinase (p160ROCK)-regulated neurite remodeling in neuroblastoma N1E-115 cells. J. Cell Biol. *141*, 1625–1636.

Ishizaki, T., Maekawa, M., Fujisawa, K., Okawa, K., Iwamatsu, A., Fujita, A., Watanabe, N., Saito, Y., Kakizuka, A., Morii, N., and Narumiya, S. (1996). The small GTP-binding protein Rho binds to and activates a 160 kDa Ser/Thr protein kinase homologous to myotonic dystrophy kinase. EMBO J. *15*, 1885–1893.

Ishizaki, T., Naito, M., Fujisawa, K., Maekawa, M., Watanabe, N., Saito, Y., and Narumiya, S. (1997). p160ROCK, a Rho-associated coiled-coil forming protein kinase, works downstream of Rho and induces focal adhesions. FEBS Lett. *404*, 118–124.

Jin, Z., and Strittmatter, S.M. (1997). Rac1 mediates collapsin-1-induced growth cone collapse. J. Neurosci. *17*, 6256–6263.

Katoh, H., Aoki, J., Ichikawa, A., and Negishi, M. (1998). p160 RhoA-binding kinase ROKα induces neurite retraction. J. Biol. Chem. *273*, 2489–2492.

Kaufmann, N., Wills, Z.P., and Van Vactor, D. (1998). Drosophila Rac1 controls motor axon guidance. Development *125*, 453–461.

Kozma, R., Sarner, S., Ahmed, S., and Lim, L. (1997). Rho family GTPases and neuronal growth cone remodelling: relationship between increased complexity induced by Cdc42Hs, Rac1, and acetylcholine and collapse induced by RhoA and lysophosphatidic acid. Mol. Cell Biol. *17*, 1201–1211.

Krendel, M., Gloushankova, N.A., Bonder, E.M., Feder, H.H., Vasiliev, J.M., and Gelfand, I.M. (1999). Myosin-dependent contractile activity of the actin cytoskeleton modulates the spatial organization of cell-cell contacts in cultured epitheliocytes. Proc. Natl. Acad. Sci. USA *96*, 9666–9670.

Lamoureux, P., Altun-Gultekin, Z.F., Lin, C., Wagner, J.A., and Heidemann, S.R. (1997). Rac is required for growth cone function but not neurite assembly. J. Cell Sci. *110*, 635–641.

Lang, P., Gesbert, F., Delespine-Carmagnat, M., Stancou, R., Pouchelet, M., and Bertoglio, J. (1996). Protein kinase A phosphorylation of RhoA mediates the morphological and functional effects of cyclic AMP in cytotoxic lymphocytes. EMBO J. *15*, 510–519.

Lee, T., Winter, C., Marticke, S.S., Lee, A., and Luo, L. (2000). Essential roles of drosophila RhoA in the regulation of neuroblast proliferation and dendritic but not axonal morphogenesis. Neuron *25*, 307–316.

Lehmann, M., Fournier, A., Selles-Navarro, I., Dergham, P., Sebok, A., Leclerc, N., Tigyi, G., and McKerracher, L. (1999). Inactivation of rho signaling pathway promotes CNS axon regeneration. J. Neurosci. *19*, 7537–7547.

Leung, T., Chen, X.Q., Manser, E., and Lim, L. (1996). The p160 RhoA-binding kinase ROK alpha is a member of a kinase family and is involved in the reorganization of the cytoskeleton. Mol. Cell Biol. *16*, 5313–5327.

Li, Z., Van Aelst, L., and Cline, H.T. (2000). Rho GTPases regulate distinct aspects of dendritic arbor growth in Xenopus central neurons in vivo. Nat. Neurosci. *3*, 217–225.

Lim, L., Manser, E., Leung, T., and Hall, C. (1996). Regulation of phosphorylation pathways by p21 GTPases. The p21 Ras-related Rho subfamily and its role in phosphorylation signaling pathways. Eur. J. Biochem. *242*, 171–185.

Lindner, J., Orkand, P.M., and Schachner, M. (1985). Histotypic pattern formation in cerebellar reaggregate cultures in the presence of antibodies to L1 cell surface antigen. Neurosci. Lett. *55*, 145–149.

Liu, J.P., and Jessell, T.M. (1998) A role for rhoB in the delamination of neural crest cells from the dorsal neural tube. Development *125*, 5055–5067.

Luo, L., Hensch, T.K., Ackerman, L., Barbel, S., Jan, L.Y., and Jan, Y.N. (1996). Differential effects of the Rac GTPase on Purkinje cell axons and dendritic trunks and spines. Nature *379*, 837–840.

Luo, L., Liao, Y.J., Jan, L.Y., and Jan, Y.N. (1994). Distinct morphogenetic functions of similar small GTPases: Drosophila Drac1 is involved in axonal outgrowth and myoblast fusion. Genes Dev. *8*, 1787–1802.

Maekawa, M., Ishizaki, T., Boku, S., Watanabe, N., Fujita, A., Iwamatsu, A., Obinata, T., Ohashi, K., Mizuno, K., and Narumiya, S. (1999). Signaling from Rho to the actin cytoskeleton through protein kinases ROCK and LIM-kinase. Science *285*, 895–898.

Matsui, T., Amano, M., Yamamoto, T., Chihara, K., Nakafuku, M., Ito, M., Nakano, T., Okawa, K., Iwamatsu, A., and Kaibuchi, K. (1996). Rho-associated kinase, a novel serine/threonine kinase, as a putative target for small GTP binding protein Rho. EMBO J. *15*, 2208–2216.

Nakayama, A., Harms, M.B., and Luo, L. (2000). Small GTPases Rac and Rho in the maintenance of dendritic spines and branches in hippocampal pyramidal neurons. J. Neurosci., in press.

Narumiya, S., Ishizaki, T., and Watanabe, N. (1997). Rho effectors and reorganization of actin cytoskeleton. FEBS Lett. *410*, 68–72.

Nikolic, M., Chou, M.M., Lu, W., Mayer, B.J., and Tsai, L.H. (1998). The p35/Cdk5 kinase is a neuron-specific Rac effector that inhibits Pak1 activity. Nature *395*, 194–198.

Ohashi, K., Nagata, K., Maekawa, M., Ishizaki, T., Narumiya, S., and Mizuno, K. (2000). Rho-associated kinase ROCK activates LIM-kinase 1 by phosphorylation at threonine 508 within the activation loop. J. Biol. Chem. *275*, 3577–3582.

Powell, S.K., Rivas, R.J., Rodriguez-Boulan, E., and Hatten, M.E. (1997). Development of polarity in cerebellar granule neurons. J. Neurobiol. *32*, 223–236.

Rivas, R.J., and Hatten, M.E. (1995). Motility and cytoskeletal organization of migrating cerebellar granule neurons. J. Neurosci. *15*, 981–989.

Ruchhoeft, M.L., Ohnuma, S., McNeill, L., Holt, C.E., and Harris, W.A. (1999). The neuronal architecture of Xenopus retinal ganglion cells is sculpted by Rho-family GTPases in vivo. J. Neurosci. *19*, 8454–8463.

Sebok, A., Nusser, N., Debreceni, B., Guo, Z., Santos, M.F., Szeberenyi, J., and Tigyi, G. (1999). Different roles for RhoA during neurite initiation, elongation, and regeneration in PC12 cells. J. Neurochem. *73*, 949–960.

Shibasaki, Y., Ishihara, H., Kizuki, N., Asano, T., Oka, Y., and Yazaki, Y. (1997). Massive actin polymerization induced by phosphatidylinositol-4-phosphate 5-kinase in vivo. J. Biol. Chem. *272*, 7578–7581.

Sone, M., Hoshino, M., Suzuki, E., Kuroda, S., Kaibuchi, K., Nakagoshi, H., Saigo, K., Nabeshima, Y., and Hama, C. (1997). Still life, a protein in synaptic terminals of Drosophila homologous to GDP-GTP exchangers. Science *275*, 543–547.

Steven, R., Kubiseski, T.J., Zheng, H., Kulkarni, S., Mancillas, J., Ruiz Morales, A., Hogue, C.W., Pawson, T., and Culotti, J. (1998). UNC-73 activates the Rac GTPase and is required for cell and growth cone migrations in C. elegans. Cell *92*, 785–795.

Sumi, T., Matsumoto, K., Takai, Y., and Nakamura, T. (1999). Cofilin phosphorylation and actin cytoskeletal dynamics regulated by rho- and Cdc42-activated LIM-kinase 2. J. Cell Biol. *147*, 1519–1532.

Tanaka, E., and Sabry, J. (1995). Making the connection: cytoskeletal rearrangements during growth cone guidance. Cell *83*, 171–176.

Tassabehji, M., Metcalfe, K., Fergusson, W.D., Carette, M.J., Dore, J.K., Donnai, D., Read, A.P., Proschel, C., Gutowski, N.J., Mao, X., and Sheer, D. (1996). LIM-kinase deleted in Williams syndrome. Nat. Genet. *13*, 272–273.

Tessier-Lavigne, M., and Goodman, C.S. (1996). The molecular biology of axon guidance. Science *274*, 1123–1133.

Threadgill, R., Bobb, K., and Ghosh, A. (1997). Regulation of dendritic growth and remodeling by Rho, Rac, and Cdc42. Neuron *19*, 625–634.

Uehata, M., Ishizaki, T., Satoh, H., Ono, T., Kawahara, T., Morishita, T., Tamakawa, H., Yamagami, K., Inui, J., Maekawa, M., and Narumiya, S. (1997). Calcium sensitization of smooth muscle mediated by a Rho-associated protein kinase in hypertension. Nature *389*, 990–994.

Van Vactor, D., and Flanagan, J.G. (1999). The middle and the end: slit brings guidance and branching together in axon pathway selection. Neuron *22*, 649–652.

Witke, W., Podtelejnikov, A.V., Di Nardo, A., Sutherland, J.D., Gurniak, C.B., Dotti, C., and Mann, M. (1998). In mouse brain profilin I and profilin II associate with regulators of the endocytic pathway and actin assembly. EMBO J. *17*, 967–976.

Yamashita, T., Tucker, K.L., and Barde, Y.A. (1999). Neurotrophin binding to the p75 receptor modulates Rho activity and axonal outgrowth. Neuron *24*, 585–593.

Yang, N., Higuchi, O., Ohashi, K., Nagata, K., Wada, A., Kangawa, K., Nishida, E., and Mizuno, K. (1998). Cofilin phosphorylation by LIM-kinase 1 and its role in Rac-mediated actin reorganization. Nature *393*, 809–812.

Zipkin, I.D., Kindt, R.M., and Kenyon, C.J. (1997). Role of a new Rho family member in cell migration and axon guidance in C. elegans. Cell *90*, 883–894.